

41. TRIASSIC (UPPER CARNIAN–LOWER RHAETIAN) MAGNETOSTRATIGRAPHY OF LEG 122 SEDIMENTS, WOMBAT PLATEAU, NORTHWEST AUSTRALIA¹

Bruno Galbrun²

ABSTRACT

During drilling at Sites 759, 760, and 761 of Leg 122 (Exmouth Plateau, northwest Australia), a thick section of Upper Triassic sediments was recovered. Paleomagnetic analyses were made on 398 samples from Holes 759B, 760A, 760B, and 761C. Progressive thermal demagnetization, alternating field demagnetization, or mixed treatment removed an initial unstable component and isolated a characteristic remanent magnetization which is of normal or reversed polarity. The magnetostratigraphic results allow us to propose a magnetic polarity sequence which extends from the upper Carnian to lower Rhaetian. This sequence reveals many more reversals than previously suggested from paleomagnetic studies. The magnetostratigraphic data also allow us to suggest correlations between Sites 759 and 760.

INTRODUCTION

One of the major objectives of Leg 122 was to refine the Mesozoic geological time scale. The unexpected recovery of an Upper Triassic sequence during Leg 122 on the Exmouth Plateau (northwest Australia) offered us the opportunity to specify the magnetic polarity sequence of this period.

A 900-m-thick sequence of Triassic (upper Carnian through lower Rhaetian) sediments was cored at four sites (Sites 759, 760, 761, and 764) on the Wombat Plateau, a small subplateau of the northern Exmouth Plateau (Fig. 1). The composite section recovered at these four sites comprises (1) a paralic to marginal-marine, middle Carnian–Norian section of an early rift environment, and (2) an almost complete marine Rhaetian carbonate platform sequence. The oldest sediments recovered are of middle Carnian age (Site 759), and represent the oldest marine sediments recovered by scientific ocean drilling. Spores and pollens proved to be the best source of age information for the Triassic.

The objective of this study was to obtain a detailed magnetostratigraphy for each site. We report here the results obtained from Holes 759B, 760A, 760B, and 761C. These data allow us to present a magnetic polarity sequence from upper Carnian through lowermost Rhaetian, and to suggest correlations between Sites 759 and 760.

SAMPLING AND MEASUREMENTS

All of the archive sections of cores from Holes 759B, 760A, 760B, and 761C were measured on board using the pass-through cryogenic magnetometer. The natural remanent magnetization (NRM) intensities range through a broad interval from sedimentary units too weakly magnetized to be measured, to very highly magnetized sections of Holes 760A and 760B. Given these problems of NRM intensity, severe core disturbance of some soft sediments, and magnetic overprinting (the 9-mT alternating field demagnetization provided by the pass-through cryogenic magnetometer was often insuffi-

cient to remove all of the secondary overprint), the whole-core measurements generally proved of little practical use. Thus, extended sampling was performed for shore-based analysis.

Two or three oriented samples were collected from each 1.5-m section of recovered sedimentary rocks. In soft sediments, such as claystones, oriented specimens (7 cm³) were cut from the working half of the split core, placed in plastic sample boxes, and capped. In indurated sediments, such as limestones or siltstones, oriented minicores were drilled perpendicular to the axis of the split core with a water-lubricated drill press. All samples were scored with a vertical orientation mark.

Measurements of the material were made on a 3-axis RS-01 (LETI/CEA) cryogenic magnetometer (Département de Géologie Sédimentaire, Université Paris VI). The background noise level of this instrument is such that it could measure samples as weakly magnetized as 2×10^{-5} A/m with good precision. For samples with an intensity of magnetization less than 10^{-5} A/m, the imprecision is too great and such measurements were rejected as unreliable indicators of the polarity.

Thermal demagnetization, alternating field (AF) demagnetization, and mixed treatment (moderate heating and subsequent AF demagnetization), which is very effective for old sedimentary rocks (Daly, 1981; Galbrun et al., 1988), were used to isolate stable remanence. AF demagnetization was performed on a single-axis Schonstedt AF demagnetizer. The most weakly magnetized samples could not be demagnetized at high fields because of acquisition of anhysteretic remanent magnetization (ARM) components caused by the demagnetizer. Thermal demagnetization was done in a furnace with a separate cooling chamber. Friable samples were enclosed in aluminium foil in order to avoid splitting during heating. The direction of characteristic magnetization was computed on each sample by an analysis of remanent magnetization directions during demagnetization treatment and by applying a least-squares line fit to the region of stability after the removing of unstable overprinting (Kirschvink, 1980). For samples that could not be demagnetized at high steps (given NRM intensity weakness, magnetic alteration during thermal demagnetization, or ARM effect during AF demagnetization), the characteristic direction was defined at the last step measured with good precision during the demagnetization.

¹ von Rad, U., Haq, B. U., et al., 1992. *Proc. ODP, Sci. Results*, 122: College Station, TX (Ocean Drilling Program).

² Université Paris VI, Département de Géologie Sédimentaire, UA-CNRS 1315, 4 place Jussieu, 75252 Paris cedex 05, France.

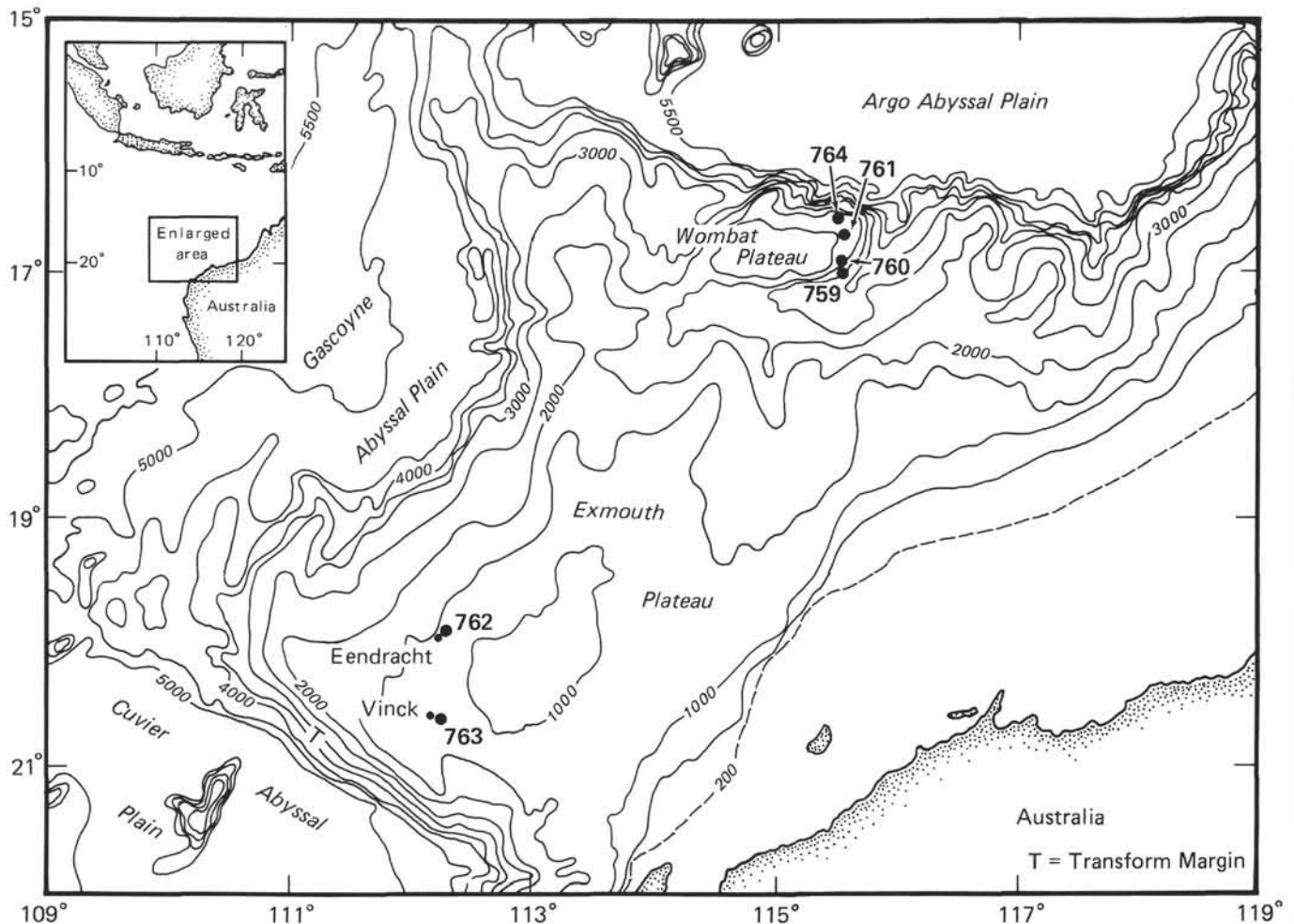


Figure 1. Bathymetric map of Exmouth Plateau with location of Leg 122 sites. Bathymetry in meters.

Since borehole cores were not oriented azimuthally, only inclination values were used for polarity interpretation. In the Southern Hemisphere, negative inclinations result from a normal polarity, positive inclinations from a reversed polarity.

MAGNETIC PROPERTIES AND POLARITY INTERPRETATION

Site 759

Site 759 is located on the southeastern flank of Wombat Plateau (16°57'S, 115°33'E). The Upper Triassic stratigraphic succession from Hole 759B consists of three units. The oldest, Unit V (205.0–308.0 mbsf), consists of a sequence of laminated silty claystones, bioturbated mudstones, siltstones, and sandstones (Shipboard Scientific Party, 1990a). This unit is of Carnian age. Unit IV (135.9–205.0 mbsf) consists of interbedded, neritic carbonates and dark gray, silty claystones. Unit III consists of alternating neritic carbonates and paralic claystones of Norian age.

A total of 145 samples were taken from Hole 759B. The claystones and silty claystones of Unit V have an NRM intensity ranging from 10^{-4} to 2.67×10^{-3} A/m. Units IV and III, which comprise some neritic carbonates, are less magnetized and some samples have an NRM intensity weaker than 10^{-4} A/m.

Seven pilot samples were progressively AF demagnetized in peak fields of 5, 10, 15, 20, 25, 30, 40, and 50 mT. This treatment was effective in removing a secondary soft compo-

nent in 15–20 mT peak fields and in defining a vector at higher fields that demagnetized to give a fairly linear segment toward the origin of a vector diagram (Fig. 2A). Thirty-four samples were thermally demagnetized up to 450°C. This technique was reasonably effective in removing secondary magnetization by 200°–240°C heating and isolating a stable component (Fig. 2B). But most of the samples become viscous after heating at 300°C and some magnetic alterations occurred. This phenomenon of magnetic alteration during high temperature heating is very common in sedimentary rocks (Lowrie and Heller, 1982). On the basis of the pilot studies all the remaining samples were demagnetized by a mixed treatment. Fifty-three soft sediment samples in plastic boxes were heated at 100°C (above 100°C the plastic boxes melt), and then AF demagnetized to a peak field value of 35 or 40 mT. Fifty-one minicores were heated at 150° and/or 210°C (these applications of heat were effective in removing most of the secondary component), and then demagnetized by AF to a peak field value of 35 or 40 mT. These mixed treatments were also effective in isolating a stable component (Figs. 2C and 2D). This stable component is of negative or positive inclination and thus is most probably a primary component.

The direction of the characteristic remanent magnetization (ChRM) of each sample was computed by applying a three dimensional least-squares line fit technique to vectors in the region of linear decay toward the origin of the vector plot. The set of vectors used for this analysis varied from sample to sample

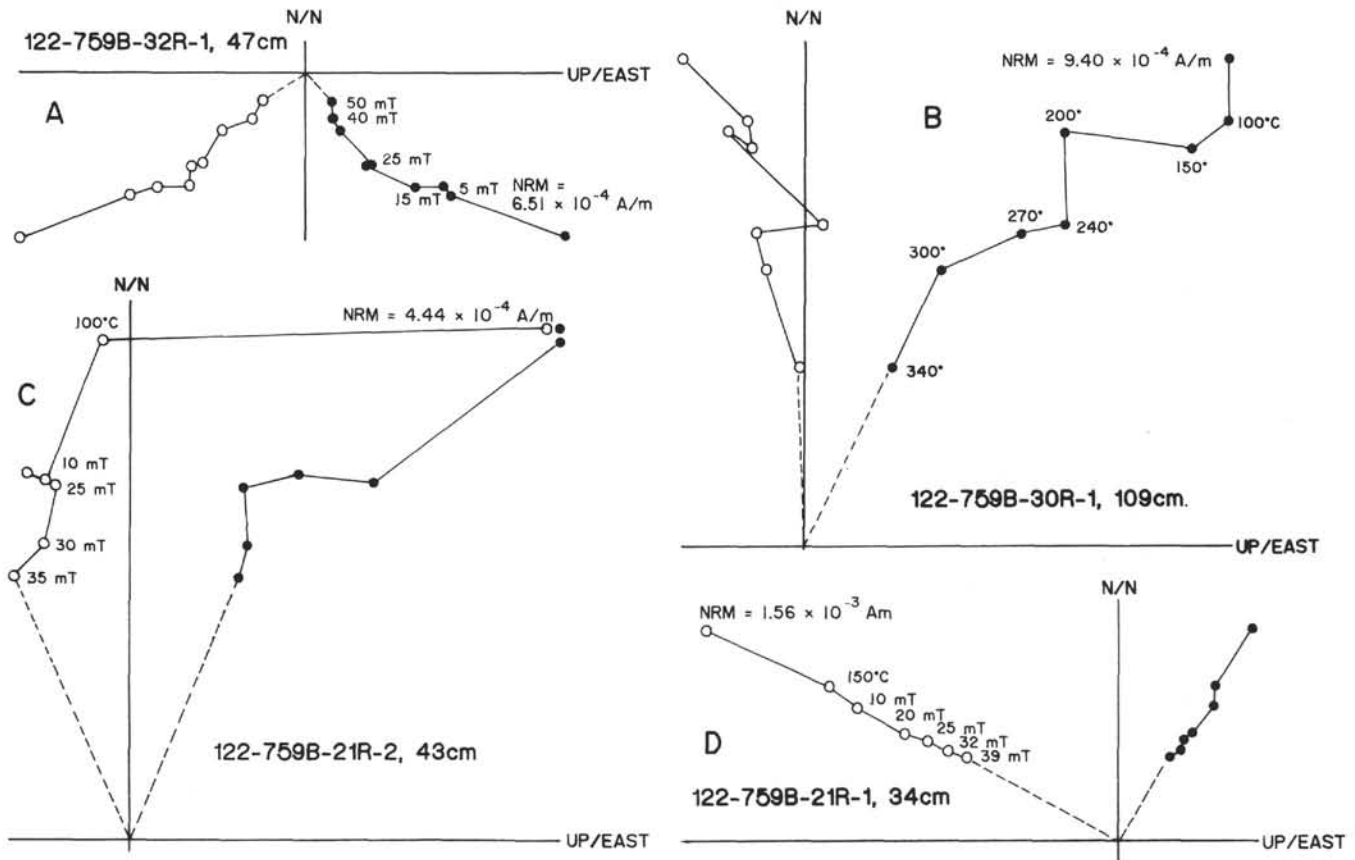


Figure 2. Representative demagnetization diagrams of Hole 759B samples. A. AF demagnetization. B. Thermal demagnetization. C, D. Mixed cleaning. Solid circles denote projection in the vertical (horizontal) plane. The initial declination is arbitrary because orientation control is lacking.

depending on the treatment used (AF, thermal, or mixed). Some samples do not reach a linear decay to the origin of the vector plot. They either had too weak an NRM intensity to be demagnetized at a field intensity or temperature sufficient to remove all the secondary component, or they acquired an ARM component during AF demagnetization. Only those samples that were sufficiently demagnetized to reveal their true polarity were considered. Of these, the ChRM direction was defined as the last direction measured with good precision.

The ChRM directions plotted against depth allow us to propose a magnetic polarity sequence for Hole 759B (Fig. 3). This sequence is dominated by normal polarity except in its uppermost part, which seems to be of reversed polarity (tops of Cores 122-759B-6R, -7R, and -8R), but the polarity cannot be positively determined because the recovery at the top of Hole 759B was very poor (2% to 30%). From Cores 122-759B-11R through -25R, the recovery is also poor (up to 50% only), and the polarity is normal except for short reversed-polarity zones defined by single samples. The lower part of the hole was well recovered (Cores 122-759B-26R through -39R) and the polarity sequence is well defined. It is of normal polarity with three short reversed magnetozones and four others that are defined by single samples.

Thus the upper Carnian-lower Norian of Hole 759B yielded a good magnetostratigraphic record.

Site 760

Site 760 is located 5 km north of Site 759 at the top of Wombat Plateau (16°55'S, 115°34'E). We drilled 422 m of

Triassic rocks (upper Carnian to Norian). The sediments recovered from Holes 760A and 760B consist mainly of silty claystones, clayey siltstones, and silty sandstones, except in Unit VI (284.9–464.05 mbsf) in which some fossiliferous limestones are interbedded (Shipboard Scientific Party, 1990b).

We studied 211 samples from Holes 760A and 760B. The NRM intensities range from 4.70×10^{-5} to 7.18×10^{-3} A/m, but most of the samples have intensities ranging from 10^{-4} to 10^{-3} A/m.

A pilot set of 10 samples was measured on board with the spinner magnetometer. An initial soft component of the NRM was removed at 5 mT. Above this field a stable component of normal or reversed polarity was isolated (Shipboard Scientific Party, 1990b). Eight samples were treated thermally in 50°C steps up to 400°C. An initial unstable component was removed by 250°C (Fig. 4A). The characteristic magnetization is clearly defined above this temperature. But thermal demagnetization was complicated by creation of a new magnetic mineral during heating: the samples become very viscous above 350°C. This effect, very common in sedimentary rocks, is due to the destruction of clay minerals.

Given these pilot studies all of the remaining samples were analyzed by mixed demagnetization (thermal and AF). Fifty-four soft sediments in plastic boxes were heated at 100°C and AF demagnetized. One-hundred thirty-nine indurated mini-cores were thermally demagnetized at various temperatures (150° and 210°C, or 250°C) and subjected to subsequent AF demagnetization. All these mixed treatments were effective in

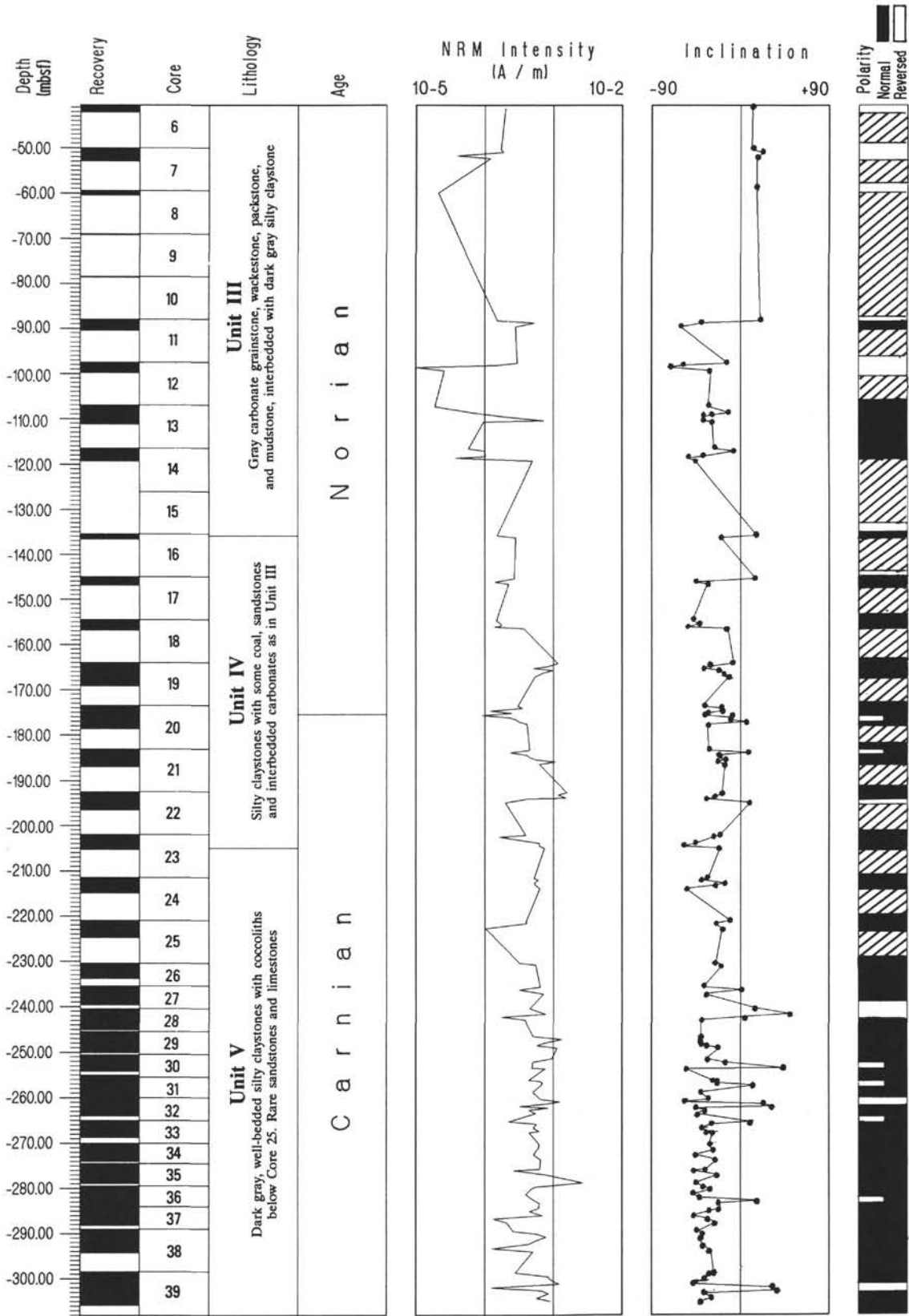


Figure 3. Magnetostratigraphic results from Hole 759B, showing depth, recovery (black), cores, lithological units, age, NRM intensity, inclination, and polarity interpretation (black = normal polarity, white = reversed polarity, and hatched areas = no polarity information owing to poor recovery).

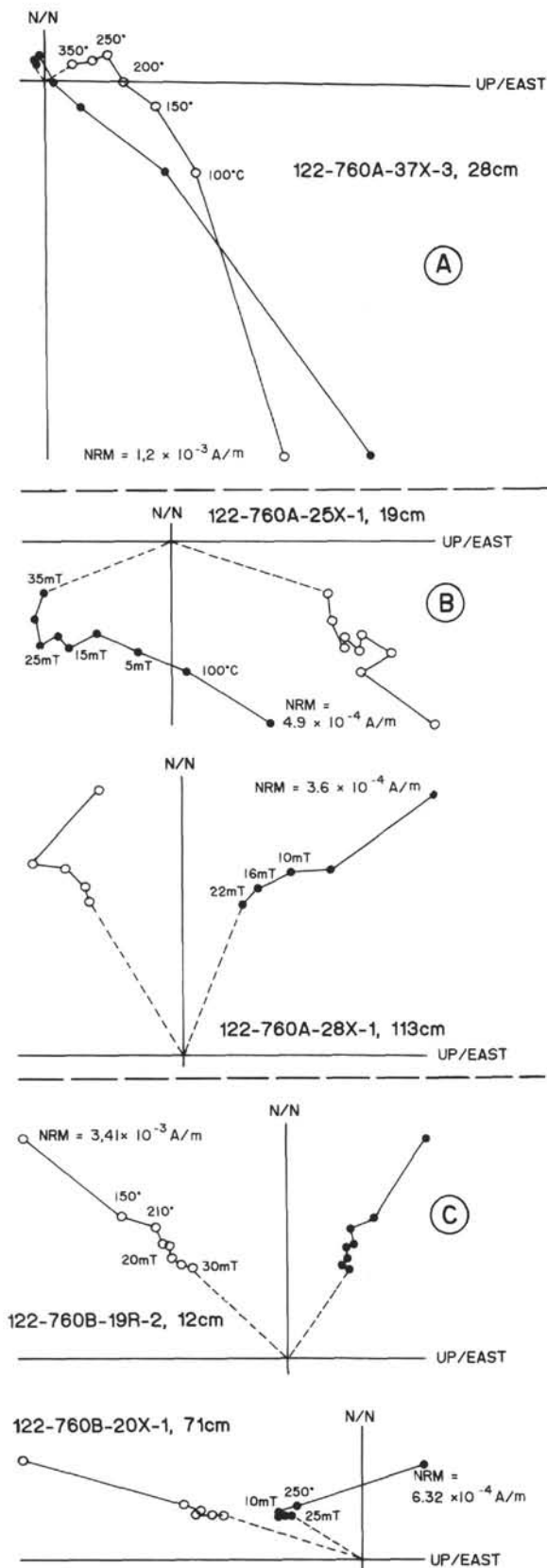


Figure 4. Representative demagnetization diagrams of samples from Holes 760A and 760B. A. Thermal demagnetization. B. Mixed treatment (100°C and AF demagnetization) on soft samples in plastic boxes. C. Mixed treatment (150°C, 210°C, or 250°C, and AF demagnetization) on indurated minicores.

removing the secondary component and in isolating the primary magnetization (Figs. 4B and 4C). The ChRM directions were computed using the same technique as for Site 759.

The characteristic magnetization directions are presented in Figures 5 and 6 for Holes 760A and 760B, respectively. They define good magnetic polarity sequences, although the recovery was sometimes poor.

Site 761

Site 761 is located on the central part of Wombat Plateau (16°44'S, 115°32'E). We penetrated 162.9 m of Triassic sediments in Hole 761C (Shipboard Scientific Party, 1990c). The upper part of this sedimentary sequence (Unit IV, 259.5–338.3 mbsf) consists of 78.8 m of white shallow-water limestones of Rhaetian age. Subunit Va (338.3–399.3 mbsf) is a 61.0-m-thick sequence of very dark gray to black marine limestones with calcareous claystones. Below these are 23.1 m of dark calcareous claystones alternating with crinoidal limestones (Subunit Vb, 399.3–422.4 mbsf). Only 2.6 m of sediments (Core 122-761C-33R) were recovered from the black Norian siltstones and claystones of Unit VI (422.4–436.7 mbsf).

Unit IV was poorly recovered (less than 8%) and thus not sampled. Forty-two samples were studied from Cores 122-761C-23R through -33R (Units V and VI). The NRM intensities of siltstones and claystones of Unit VI and calcareous claystones of Subunit Vb range from 3.3×10^{-5} to 1.6×10^{-3} A/m. The sediments of Subunit Va, on which the relative proportion of carbonates to terrigenous sediments is more important, have weaker NRM intensities, ranging from 1.3×10^{-5} to 1.7×10^{-4} A/m.

Thirty-four indurated minicores were subjected to progressive thermal demagnetization at 50°C increments from 100° to 400°C. A first soft component is removed by 200°C heating (Fig. 7A). During further thermal cleaning the magnetization vector decays univectorially toward the origin of the projection; thus, a stable component of negative or positive inclination is easily determined. However, some erratic changes in direction and NRM intensity occur above 350°C in most samples. This change is attributed to the destruction of clay minerals and formation of a new magnetic mineral. Thus only a few samples were heated above 300°C. Eight soft samples in plastic boxes were heated at 100°C and AF-demagnetized to peak fields of 10, 15, 20, and 25 mT. This mixed treatment was also effective in removing the soft secondary component above 10 mT (Fig. 7B).

The characteristic remanent magnetization directions define a magnetic polarity sequence which is presented in Figure 8. Three samples from Cores 122-761C-23R and -24R were too weakly magnetized and no characteristic direction could be computed on these samples. The magnetic polarity sequence shows an alternation of normal and reversed zones, most of which are defined by two or more samples. Five short polarity zones are established by single samples.

DISCUSSION AND CONCLUSION

The Upper Triassic magnetic polarity sequence is not well known (Haq et al., 1987). Few magnetostratigraphic studies have been carried out on sections of this age and none having ammonite or conodont biostratigraphy, although these groups of fossils are used to define the boundary stages of the Upper Triassic.

Some paleomagnetic studies of Upper Triassic continental sedimentary or volcanic rocks in North America (Reeve and Helsley, 1972; Steiner and Helsley, 1974) have yielded magnetostratigraphic results. The Upper Triassic Kayenta Formation (Utah) reveals four normal and four reversed intervals of polarity (Steiner and Helsley, 1974), but the age of this formation is now regarded as Lower Jurassic considering

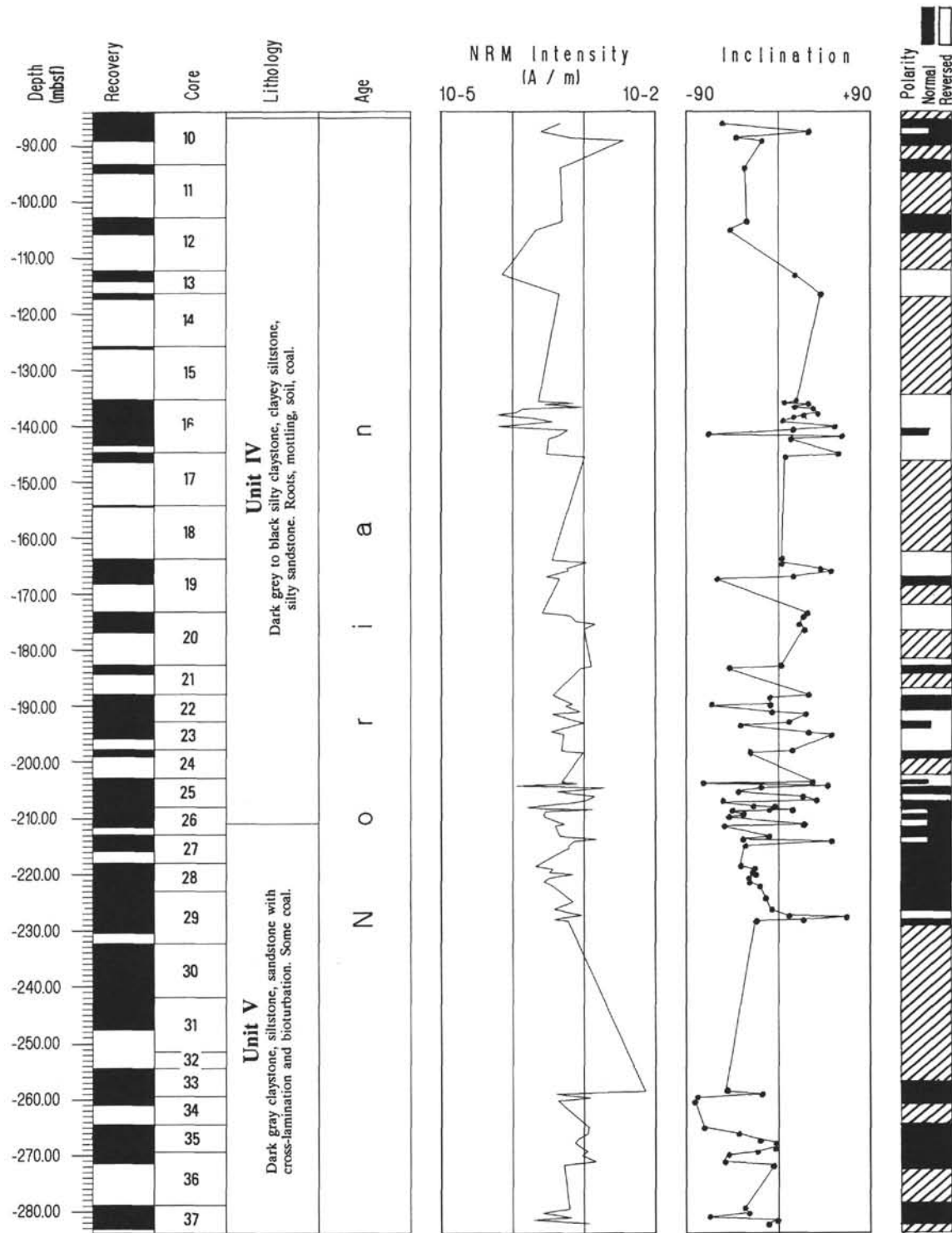


Figure 5. Magnetostratigraphic results from Hole 760A. (See Fig. 3 caption for details.)

biostratigraphic data (Podian, 1989). The upper portion of the Chinle Formation (New Mexico) reveals at least eight polarity intervals (Reeve and Helsley, 1972), but this formation is poorly dated. The Newark Basin (Pennsylvania) was intensively studied for paleomagnetic and magnetostratigraphic purposes (McIntosh et al., 1985; Witte and Kent, 1989; Olsen and Kent, 1990). From these studies it appears that the Stockton and Lockatong Formations of the upper Carnian are

of reversed polarity. The Passaic Formation (uppermost Carnian–Norian) presents four intervals of normal polarity of which the oldest is uppermost Carnian.

Despite incomplete core recovery, the magnetostratigraphic data obtained from Leg 122 allow us to propose a magnetic polarity sequence which extends from the upper Carnian to lowermost Rhaetian (Fig. 9). It appears that the uppermost Carnian is mainly of normal polarity with some

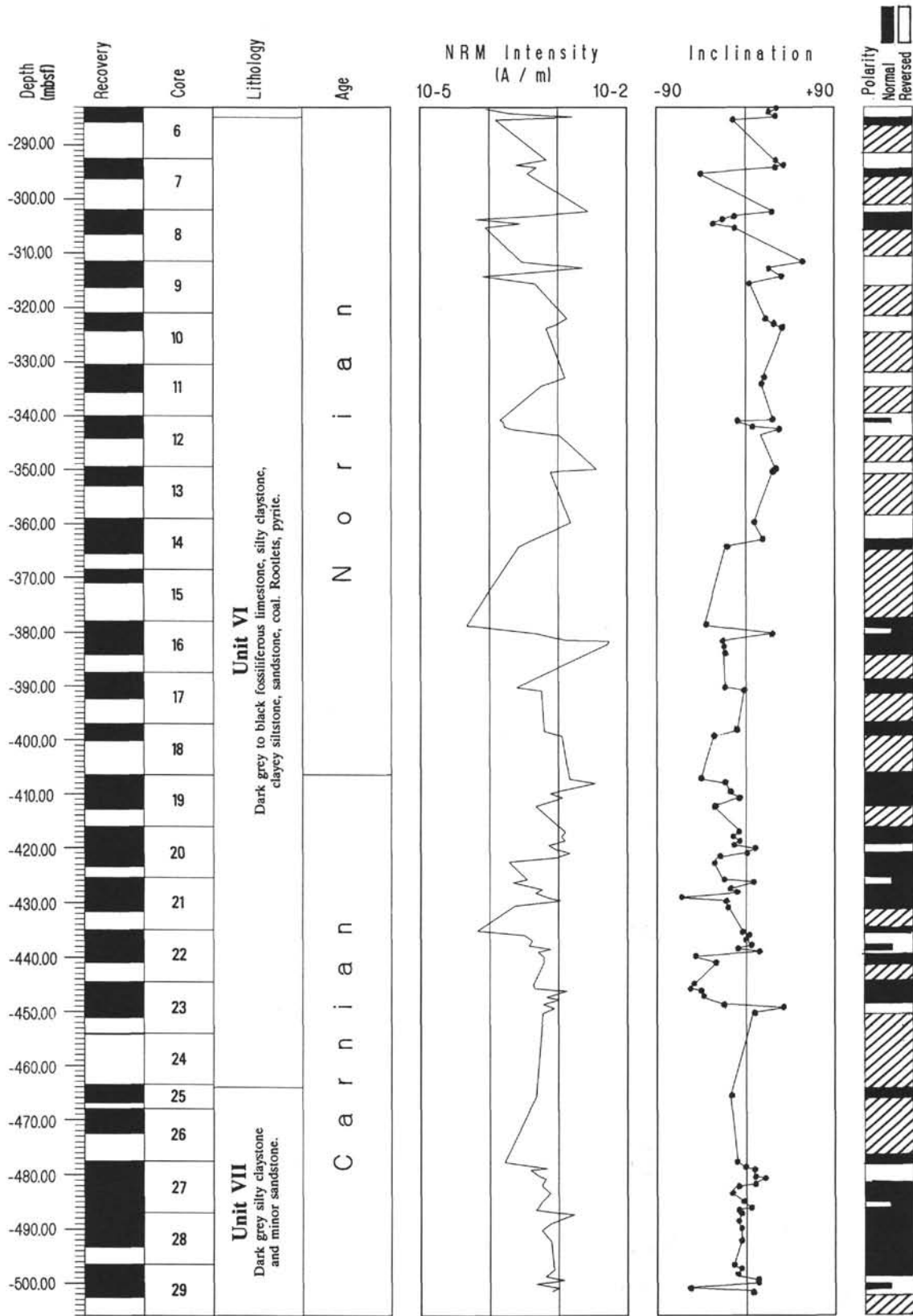


Figure 6. Magnetostratigraphic results from Hole 760B. (See Fig. 3 caption for details.)

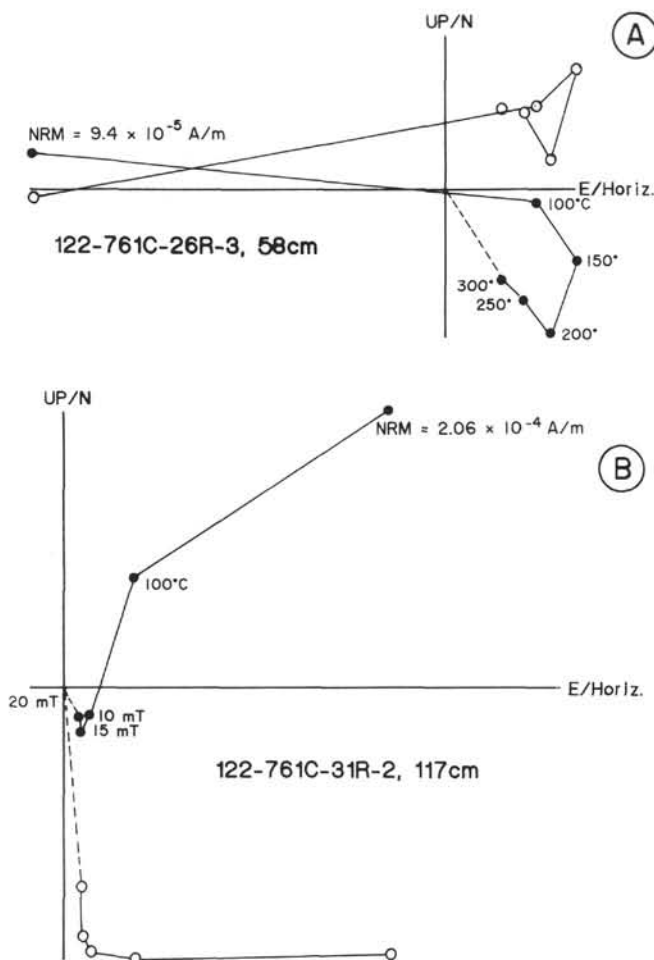


Figure 7. Representative demagnetization diagrams on Hole 761C samples. A. Thermal demagnetization. B. Mixed treatment.

short reversed polarity events. But most of these events are defined by single samples. The lowermost Norian is of normal polarity, then a 50-m-thick, reversed-polarity zone occurs in the lower Norian (from Cores 122-760B-14R to -9R, Unit VI; see Fig. 6). A mixed normal-reversed sequence occurs at the top of Hole 760B. The base of Hole 760A (Unit V) is of normal polarity, but there is a gap in the sequence because Cores 122-760A-30R and -31R were not sampled. The base of Unit IV shows an increase of reversed polarity zones, and a reversed Earth's magnetic field seems predominant in the upper Norian, except in the uppermost part of this stage where the polarity becomes normal. The lower Rhaetian at Hole 761C is of mixed polarity.

Correlations between the magnetic polarity sequence derived from Leg 122 Triassic sediments and other sequences established on Upper Triassic rocks from continental basins, such as the Newark basin, are difficult because most of these results are preliminary. The biostratigraphic data are also poor. Construction of a global magnetic polarity pattern for the Upper Triassic must await additional data.

The magnetostratigraphic study of Triassic sediments recovered during Leg 122 suggests many more polarity zones from the upper Carnian through lower Rhaetian than previously established by paleomagnetic studies. This is important because the rate of magnetic field reversal fre-

quency is related to the activity of the Earth's mantle and core. For example, in the model of coupling of core and mantle convection, times of increasing reversal rate are periods of fast true polar wander (Courtilot and Besse, 1987). This model is controversial and it requires an increase in reversal frequency during the Triassic and Early Jurassic times after the Permo-Carboniferous Long Reversal Superchron. The magnetostratigraphic data of Upper Triassic sediments from Leg 122 do not allow us to confirm or invalidate this model.

Magnetostratigraphic correlations between sites are somewhat difficult to establish given the poor recovery from each hole, but some correlations between Holes 759B and 760B are suggested. We assume that there is an overlap of the two sites; an alternative hypothesis assuming a gap between the two sites was also discussed considering the poor biostratigraphic results, the seismic interpretation, and some sedimentological arguments (Shipboard Scientific Party, 1990b). The evidence for overlap comes mainly from biostratigraphy, which suggests that the age of the sediments at the bottom of Hole 760B overlap with the age of the sediments at Site 759 and that Core 122-759B-14R correlates with Core 122-760B-17R. Suggested magnetostratigraphic correlations agree well with this assessment (Fig. 9). In fact, the sequences of Cores 122-759B-12R through -39R and Cores 122-760B-16R through -29R are mainly of normal polarity. A reversed polarity zone begins in Core 122-759B-11R and extends toward the top of the hole, the same reversed zone extends at Hole 760B from Cores 122-760B-14R to -9R.

The main result of this study is its contribution to the establishment of a magnetic polarity sequence from upper Carnian to lower Rhaetian. The sequence established must be confirmed by other studies of sedimentary sections on land. This is especially necessary for all the short events, most of which are defined by single samples.

ACKNOWLEDGMENTS

I thank the Ocean Drilling Program for allowing my participation on Leg 122. The scientific party on Leg 122 aided the extensive sampling. This study was supported by ODP-France and the CNRS-UA 1315. I wish also to express my thanks to Drs. S. O'Connell and J. G. Ogg, and an anonymous referee for reviewing the manuscript. I am grateful to J. Thompson for help with the English.

REFERENCES

- Courtilot, V., and Besse, J., 1987. Magnetic field reversals, polar wander, and core-mantle coupling. *Science*, 237:1140-1147.
- Daly, L., 1981. Des aimantations partielles aux aimantations superposées: espoirs et difficultés. *Phys. Earth Planet. Inter.*, 24:218-227.
- Galbrun, B., Gabilly, J., and Rasplus, L., 1988. Magnetostratigraphy of the Toarcian stratotype sections at Thouars and Airvault (Deux-Sèvres, France). *Earth Planet. Sci. Lett.*, 87:453-462.
- Haq, B. U., Hardenbol, J., and Vail, P. R., 1987. The chronology of fluctuating sea level since the Triassic. *Science*, 235:1156-1167.
- Kirschvink, J. L., 1980. The least-squares line and plane and the analysis of paleomagnetic data. *Geophys. J. R. Astron. Soc.*, 62:699-718.
- Lowrie, W., and Heller, F., 1982. Magnetic properties of marine limestones. *Rev. Geophys. Space Phys.*, 20:171-192.
- McIntosh, W. C., Hargraves, R. B., and West, C. L., 1985. Paleomagnetism and oxide mineralogy of Upper Triassic to Lower Jurassic red beds and basalts in the Newark Basin. *Geol. Soc. Am. Bull.*, 96:463-480.
- Olsen, P. E., and Kent, D. V., 1990. Continental coring of the Newark Rift. *Eos*, 71:385.
- Podian, K., 1989. Presence of the dinosaur *Scelidosaurus* indicates Jurassic age for the Kayenta Formation (Glen Canyon Group, northern Arizona). *Geology*, 17:438-441.

Reeve, S. C., and Helsley, C. E., 1972. Magnetic reversal sequence in the upper portion of the Chinle Formation, Montoya, New Mexico. *Geol. Soc. Am. Bull.*, 83:3795-3812.

Shipboard Scientific Party, 1990a. Site 759. In Haq, B. U., von Rad, U., O'Connell, S., et al., *Proc. ODP, Init. Repts.*, 122: College Station, TX (Ocean Drilling Program), 81-114.

_____, 1990b. Site 760. In Haq, B. U., von Rad, U., O'Connell, S., et al., *Proc. ODP, Init. Repts.*, 122: College Station, TX (Ocean Drilling Program), 115-160.

_____, 1990c. Site 761. In Haq, B. U., von Rad, U., O'Connell, S., et al., *Proc. ODP, Init. Repts.*, 122: College Station, TX (Ocean Drilling Program), 161-211.

Steiner, M. B., and Helsley, C. E., 1974. Magnetic polarity sequence of the Upper Triassic Kayenta Formation. *Geology*, 2:191-194.

Witte, W. K., and Kent, D. V., 1989. A middle Carnian to early Norian (-225 Ma) paleopole from sediments of the Newark Basin, Pennsylvania. *Geol. Soc. Am. Bull.*, 101:1118-1126.

Date of initial receipt: 15 June 1990
 Date of acceptance: 16 January 1991
 Ms 122B-150

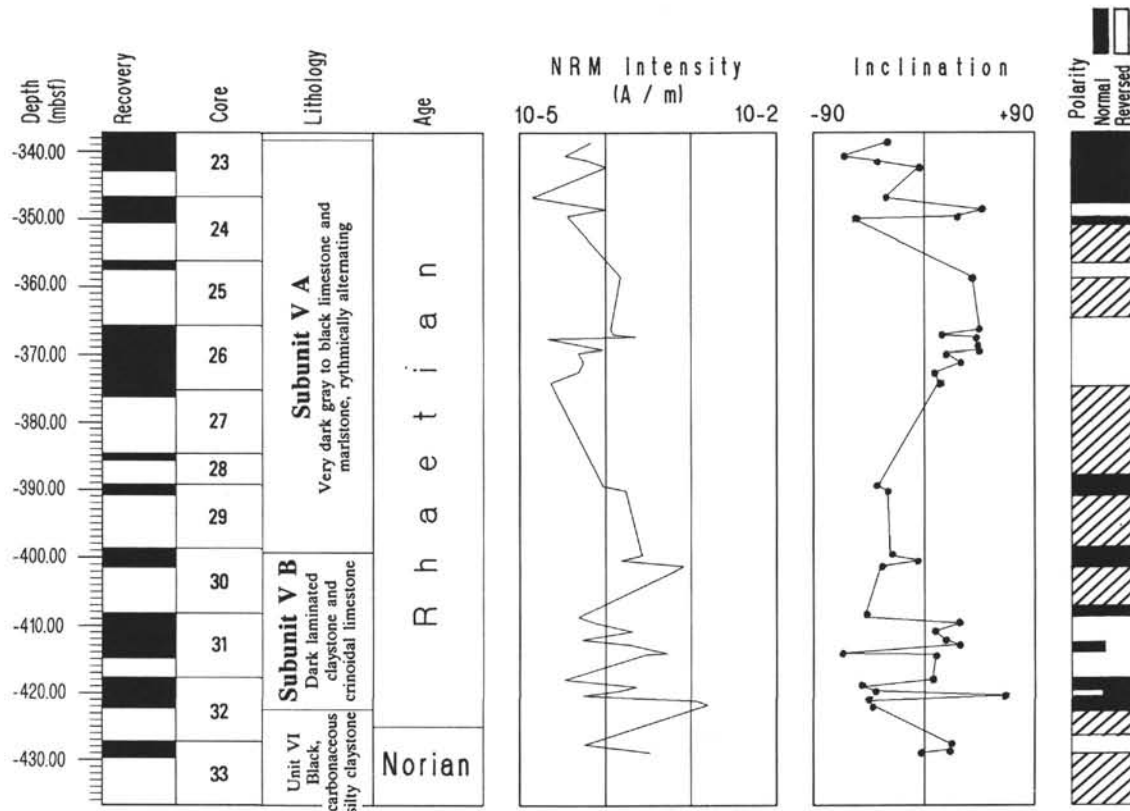


Figure 8. Magnetostratigraphic results from Hole 761C. (See Fig. 3 caption for details.)

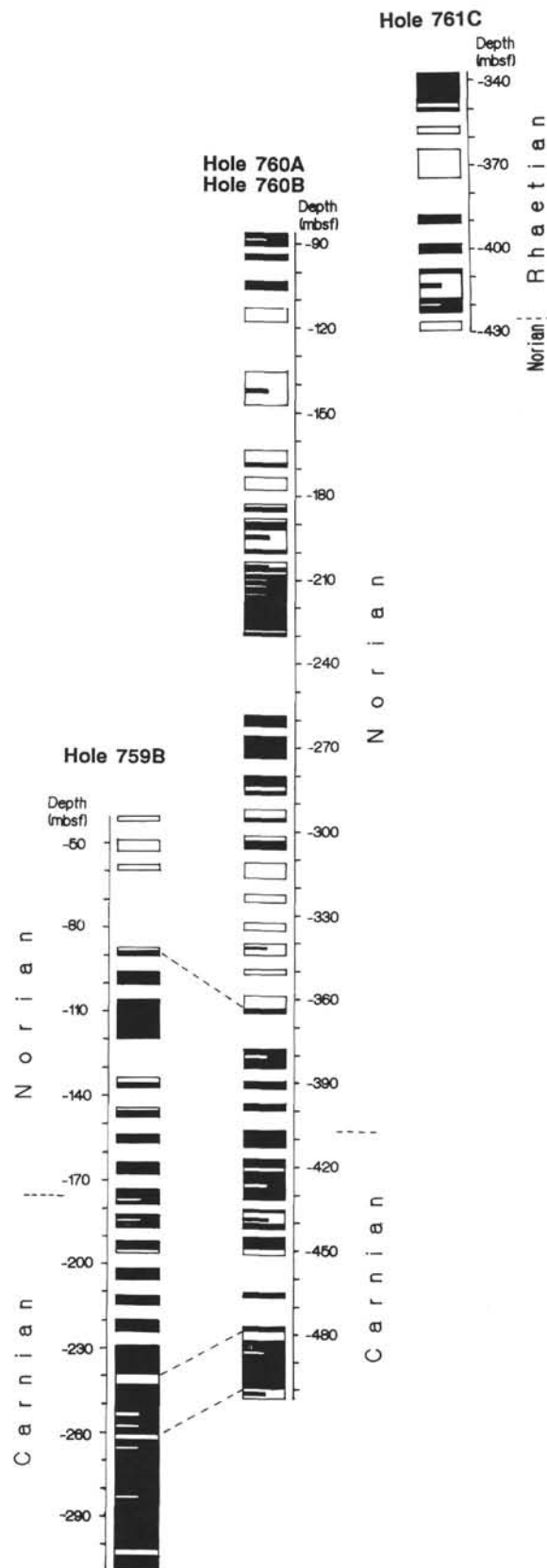


Figure 9. The three magnetic polarity sequences plotted against depth (black = normal polarity, white = reversed polarity, and short bars = single samples with polarity interpretation opposite adjacent samples). Suggested correlations between sites.

Appendix A. Directions of characteristic magnetization of Triassic sediments in Hole 759B.

Sample (core, section, cm)	Depth (mbsf)	NRM (A/m)	Inclination (°)	Demagnetization step
122-759B-				
6R-1, 80	41.30	2.01E-4	+12	100° +20mT
7R-1, 43	50.43	1.73E-4	+11	100° +15mT
7R-1, 104	51.04	1.86E-4	+22	100° +15mT
7R-2, 27	51.77	4.00E-5	+19	200°
7R-2, 88	52.38	1.20E-4	+16	320°
8R-1, 52	60.02	2.10E-5	+16	240°
11R-1, 43	88.43	1.55E-4	+20	100° +15mT
11R-1, 83	88.83	5.30E-4	-39	100° +15mT
11R-2, 27	89.77	2.81E-4	-61	360°
12R-1, 23	97.73	2.98E-4	-13	100° +25mT
12R-1, 74	98.24	1.43E-4	-59	100° +15mT
12R-1, 118	98.68	1.00E-5	-73	100° +10mT
12R-2, 38	99.38	2.60E-5	-30	280°
13R-1, 39	107.39	1.90E-5	-33	240°
13R-2, 24	108.74	6.70E-5	-12	320°
13R-2, 75	109.25	1.35E-4	-30	100° +15mT
13R-2, 114	109.64	1.96E-4	-39	100° +20mT
13R-3, 49	110.49	7.19E-4	-38	360°
13R-3, 79	110.79	9.60E-5	-29	360°
14R-1, 18	116.68	5.80E-5	-27	100° +15mT
14R-1, 65	117.15	1.00E-4	-6	100° +25mT
14R-2, 33	118.33	1.03E-4	-38	100° +15mT
14R-2, 65	118.65	3.80E-5	-54	100° +10mT
14R-2, 132	119.32	4.93E-4	-46	360°
16R-1, 46	135.96	1.51E-4	+16	320°
16R-1, 84	136.34	2.82E-4	-20	320°
17R-1, 59	145.59	2.70E-4	+15	100° +25mT
17R-1, 132	146.32	1.40E-4	-46	100° +10mT
17R-2, 22	146.72	2.22E-4	-34	100° +15mT
18R-1, 33	154.83	1.47E-4	-49	100° +10mT
18R-1, 96	155.46	1.72E-4	-43	100° +10mT
18R-1, 140	155.90	1.75E-4	-47	100° +10mT
18R-2, 21	156.21	1.38E-4	-55	100° +10mT
18R-2, 57	156.57	3.69E-4	-13	100° +25mT
19R-1, 31	164.31	1.15E-3	-7	100° +40mT
19R-1, 100	165.00	7.98E-4	-34	100° +40mT
19R-1, 142	165.42	5.12E-4	-38	100° +25mT
19R-2, 38	165.88	9.62E-4	-22	100° +40mT
19R-2, 98	166.48	6.86E-4	-18	100° +40mT
19R-3, 31	167.31	5.34E-4	-12	100° +32mT
20R-1, 26	173.76	3.03E-4	-39	100° +25mT
20R-1, 72	174.22	3.55E-4	-19	100° +25mT
20R-1, 125	174.75	1.21E-4	-18	100° +25mT
20R-2, 29	175.29	2.47E-4	-34	100° +20mT
20R-2, 76	175.76	9.20E-5	-37	100° +10mT
20R-2, 126	176.26	2.35E-4	-9	100° +10mT
20R-3, 19	176.79	2.94E-4	-11	100° +20mT
20R-3, 71	177.21	3.14E-4	+8	100° +20mT
20R-3, 122	177.72	4.14E-4	-34	100° +28mT
21R-1, 38	183.38	4.50E-4	-32	100° +28mT
21R-1, 96	183.96	2.37E-4	+8	100° +30mT
21R-1, 143	184.43	4.14E-4	-23	100° +28mT
21R-2, 43	184.93	4.44E-4	-23	100° +35mT
21R-2, 97	185.47	5.61E-4	-16	100° +40mT
21R-2, 142	185.92	1.07E-3	-24	100° +30mT
21R-3, 43	186.43	6.22E-4	-16	100° +32mT
22R-1, 34	192.84	1.57E-3	-19	150° +39mT
22R-1, 76	193.26	1.16E-3	-21	210° +25mT
22R-1, 148	193.98	1.52E-3	-28	50mT
22R-2, 22	194.22	4.25E-4	-36	250°
22R-2, 102	195.02	2.01E-4	+10	210° +25mT
23R-1, 28	202.28	3.95E-4	-21	210° +25mT
23R-1, 64	202.64	1.64E-4	-27	210° +25mT
23R-2, 47	203.97	6.25E-4	-45	250°
23R-2, 115	204.65	6.25E-4	-58	210° +25mT
23R-3, 10	205.10	7.35E-4	-21	210° +25mT
24R-1, 20	211.70	5.22E-4	-33	210° +25mT
24R-1, 63	212.13	5.96E-4	-39	100° +40mT
24R-1, 132	212.82	5.20E-4	-16	100° +32mT
24R-2, 29	213.29	5.54E-4	-26	100° +32mT
24R-2, 103	214.03	6.36E-4	-56	100° +32mT
25R-1, 15	221.15	4.03E-4	-10	100° +32mT
25R-1, 76	221.76	4.08E-4	-27	100° +25mT
25R-2, 33	222.83	1.04E-4	-19	100° +25mT

Appendix A (continued).

Sample (core, section, cm)	Depth (mbsf)	NRM (A/m)	Inclination (°)	Demagnetization step
26R-1, 3	230.53	3.21E-4	-25	250°
26R-1, 42	230.92	5.53E-4	-18	210° +25mT
27R-1, 32	235.82	6.43E-4	-38	100° +40mT
27R-1, 98	236.48	3.15E-4	+2	210° +25mT
27R-2, 41	237.41	7.14E-4	-37	210° +25mT
28R-1, 8	240.58	4.48E-4	+16	210° +25mT
28R-1, 122	241.72	7.65E-4	+50	100° +32mT
28R-2, 33	242.33	1.76E-4	+3	210° +25mT
28R-2, 99	242.99	3.87E-4	-40	250°
29R-1, 113	246.64	5.07E-4	-40	240°
29R-2, 32	247.32	1.32E-3	-41	50mT
29R-2, 108	248.08	7.33E-4	-40	270°
29R-3, 16	248.66	5.78E-4	-35	240°
29R-3, 73	249.23	1.12E-3	-21	250°
30R-1, 109	251.59	9.40E-4	-35	340°
30R-2, 28	252.28	4.99E-4	-18	270°
30R-3, 15	253.65	4.90E-4	+45	340°
30R-3, 28	253.78	7.58E-4	-56	150° +39mT
31R-1, 125	256.25	4.36E-4	-29	300°
31R-1, 145	256.45	6.13E-4	-24	300°
31R-2, 31	256.81	6.89E-4	-26	250°
31R-2, 88	257.38	6.56E-4	+15	50mT
31R-3, 90	258.90	5.04E-4	-41	300°
32R-1, 47	260.47	6.51E-4	-32	50mT
32R-1, 97	260.97	1.23E-3	-59	150° +39mT
32R-1, 142	261.42	7.87E-4	+23	300°
32R-2, 47	261.97	3.25E-4	+31	340°
32R-2, 83	262.33	8.32E-4	-46	250°
32R-2, 132	262.82	4.37E-4	-35	340°
32R-3, 58	263.58	5.55E-4	-45	210° +25mT
33R-1, 36	265.36	2.24E-4	+9	210° +25mT
33R-1, 96	265.96	5.64E-4	-30	250°
33R-2, 35	266.85	5.10E-4	-40	50mT
33R-2, 93	267.43	6.18E-4	-35	210° +25mT
33R-3, 20	267.70	4.42E-4	-28	210° +25mT
34R-1, 29	270.29	6.15E-4	-32	210° +25mT
34R-1, 120	271.20	6.07E-4	-30	210° +20mT
34R-2, 15	271.65	5.65E-4	-28	150° +39mT
34R-2, 110	272.60	5.17E-4	-46	210° +25mT
34R-3, 75	273.75	6.52E-4	-24	210° +25mT
35R-1, 130	275.80	6.31E-4	-35	210° +25mT
35R-2, 14	276.14	2.68E-4	-49	210° +25mT
35R-2, 109	277.09	7.96E-4	-23	210° +25mT
35R-3, 142	278.92	2.67E-3	-46	150° +39mT
36R-1, 31	279.81	5.39E-4	-37	50mT
36R-1, 90	280.40	4.67E-4	-30	210° +25mT
36R-2, 50	281.50	3.94E-4	-48	210° +10mT
36R-2, 114	282.14	4.51E-4	-42	210° +22mT
36R-3, 33	282.83	5.34E-4	+17	210° +22mT
36R-3, 84	283.34	6.27E-4	-21	210° +22mT
37R-1, 47	284.47	6.09E-4	-21	210° +22mT
37R-1, 115	285.15	4.47E-4	-32	210° +22mT
37R-2, 58	286.08	6.86E-4	-49	210° +22mT
37R-2, 133	286.83	1.34E-4	-33	210° +22mT
37R-3, 74	287.74	2.10E-4	-26	250°
38R-1, 64	289.64	2.58E-4	-43	210° +22mT
38R-1, 120	290.20	5.56E-4	-36	210° +22mT
38R-2, 39	290.89	7.80E-4	-39	210° +22mT
38R-2, 124	291.74	5.45E-4	-41	210° +30mT
38R-3, 44	292.44	4.42E-4	-39	210° +30mT
38R-3, 146	293.46	1.28E-4	-34	210° +30mT
38R-4, 67	294.17	5.01E-4	-30	210° +30mT
39R-1, 36	298.86	2.78E-4	-27	150° +39mT
39R-1, 118	299.68	8.31E-4	-33	210° +30mT
39R-2, 39	300.39	9.07E-4	-38	210° +30mT
39R-2, 125	301.25	1.20E-3	-48	250°
39R-3, 63	302.13	1.28E-4	+33	210° +30mT
39R-3, 125	302.75	6.64E-4	+37	50mT
39R-4, 41	303.41	8.48E-4	-38	210° +30mT
39R-4, 137	304.37	5.70E-4	-28	210° +30mT
39R-5, 48	304.98	8.89E-4	-40	210° +30mT

Note: The NRM column represents the initial NRM intensity of each sample and the demagnetization step column refers to the highest step attained during the treatment of each sample.

Appendix B. Directions of characteristic magnetization of Triassic sediments in Hole 760A.

Sample (core, section, cm)	Depth (mbsf)	NRM (A/m)	Inclination (°)	Demagnetization step
122-760A-				
10X-2, 68	85.88	4.59E-4	-56	240°+30mT
10X-3, 67	87.37	2.50E-4	+30	240°
10X-4, 25	88.45	6.24E-4	-44	240°+20mT
10X-CC, 25	88.95	3.58E-3	-16	100°+40mT
11X-1, 64	93.84	4.68E-4	-33	240°+30mT
12X-1, 68	103.38	4.94E-4	-31	100°+20mT
12X-2, 68	104.88	2.12E-4	-49	100°+30mT
13X-1, 69	112.89	7.20E-5	+16	100°+45mT
14X-1, 15	116.35	4.47E-4	+41	100°+20mT
16X-1, 33	135.53	2.31E-4	+18	100°+10mT
16X-1, 62	135.82	7.07E-4	+6	240°+25mT
16X-1, 88	136.08	2.84E-4	+30	240°+15mT
16X-1, 136	136.56	9.41E-4	+13	460°
16X-2, 24	136.94	1.40E-4	+34	240°+15mT
16X-2, 80	137.50	1.11E-4	+38	240°+15mT
16X-2, 126	137.96	6.20E-5	+24	240°+10mT
16X-3, 33	138.53	1.86E-4	+14	240°+20mT
16X-3, 103	139.23	3.59E-4	+2	240°+15mT
16X-4, 33	140.03	6.30E-5	+58	240°+15mT
16X-4, 103	140.73	5.89E-4	+7	250°+30mT
16X-5, 29	141.49	4.65E-4	-71	100°+15mT
16X-5, 57	141.77	4.25E-4	+65	100°+20mT
16X-5, 103	142.23	3.17E-4	+10	250°+30mT
17X-1, 31	145.01	3.01E-4	+61	250°+30mT
17X-1, 71	145.41	1.02E-3	+6	300°
19X-1, 31	164.01	3.54E-4	+3	250°+25mT
19X-1, 69	164.39	1.06E-3	+2	250°+25mT
19X-2, 25	165.45	5.66E-4	+40	250°+10mT
19X-2, 69	165.89	5.95E-4	+52	250°+15mT
19X-3, 25	166.95	2.97E-4	+13	250°+15mT
19X-3, 69	167.39	4.56E-4	-61	200°
20X-1, 23	173.43	2.58E-4	+28	100°+45mT
20X-1, 71	173.91	6.32E-4	+24	250°+30mT
20X-2, 28	174.98	7.67E-4	+21	250°+25mT
20X-2, 71	175.41	1.42E-3	+22	250°+30mT
20X-3, 12	176.32	9.88E-4	+24	250°+25mT
21X-1, 23	182.93	1.25E-3	+2	250°+20mT
21X-1, 68	183.38	8.82E-4	-51	250°
22X-1, 24	188.14	3.65E-4	+30	250°+30mT
22X-1, 67	188.57	4.29E-4	-9	250°+20mT
22X-2, 24	189.64	6.86E-4	-8	250°+20mT
22X-2, 67	190.07	5.54E-4	-67	250°+15mT
22X-3, 24	191.14	8.74E-4	-7	460°
22X-3, 67	191.57	3.59E-4	+28	250°+25mT
23X-1, 24	193.14	9.78E-4	+8	250°+30mT
23X-1, 67	193.57	7.48E-4	-39	250°+25mT
23X-2, 33	194.73	3.48E-4	+22	250°+20mT
23X-2, 83	195.23	5.17E-4	+53	250°+20mT
24X-1, 26	198.16	4.82E-4	+12	100°+10mT
24X-1, 60	198.50	9.52E-4	-30	100°+10mT
25X-1, 79	203.69	4.89E-4	+35	100°+45mT
25X-1, 89	203.79	7.88E-4	-74	100°+15mT
25X-1, 128	204.18	1.14E-4	+47	100°+40mT
25X-2, 22	204.62	1.93E-3	-17	100°+40mT

Appendix B (continued).

Sample (core, section, cm)	Depth (mbsf)	NRM (A/m)	Inclination (°)	Demagnetization step
25X-2, 89	205.29	4.21E-4	-42	100°+30mT
25X-3, 22	206.12	1.41E-3	+22	100°+30mT
25X-3, 89	206.79	1.06E-3	+39	100°+20mT
25X-3, 130	207.20	7.12E-4	-56	100°+16mT
25X-4, 22	207.62	3.35E-4	-35	100°+16mT
25X-4, 62	208.02	1.60E-4	-3	100°+16mT
25X-4, 89	208.29	3.02E-4	-11	100°+30mT
25X-5, 30	209.20	2.32E-4	-20	100°+22mT
25X-5, 71	209.61	2.20E-4	+18	100°+22mT
26X-1, 49	208.39	1.31E-3	+15	100°+30mT
26X-1, 87	208.77	2.90E-4	-48	100°+22mT
26X-1, 122	209.12	2.73E-4	-35	100°+16mT
26X-2, 13	209.53	2.73E-4	-37	100°+16mT
26X-2, 37	209.77	2.77E-4	-52	100°+10mT
26X-CC,12	211.02	5.31E-4	+26	100°+16mT
26X-CC,43	211.33	3.96E-4	-56	100°+30mT
27X-1, 25	213.15	4.55E-4	-8	100°+28mT
27X-1, 79	213.69	1.48E-3	-37	100°+28mT
27X-1, 119	214.09	7.20E-4	+52	100°+30mT
27X-2, 49	214.89	6.04E-4	-31	100°+20mT
27X-2, 81	215.21	6.11E-4	-34	100°+28mT
28X-1, 59	218.49	2.08E-4	-38	100°+22mT
28X-1, 113	219.03	3.58E-4	-23	100°+28mT
28X-2, 25	219.65	3.22E-4	-26	100°+20mT
28X-2, 53	219.93	6.82E-4	-24	100°+28mT
28X-2, 128	220.68	3.23E-4	-30	100°+28mT
28X-3, 35	221.25	2.73E-4	-29	100°+28mT
28X-3, 120	222.10	3.66E-4	-18	100°+28mT
29X-2, 44	224.84	6.99E-4	-11	100°+10mT
29X-3, 33	226.23	3.81E-4	-8	100°+28mT
29X-3, 139	227.29	9.29E-4	+8	300°
29X-4, 17	227.57	5.76E-4	+66	100°+16mT
29X-4, 70	228.10	3.79E-4	+18	100°+22mT
29X-4, 85	228.25	5.89E-4	-23	100°+28mT
33X-3, 115	258.55	7.18E-3	-52	100°+28mT
33X-4, 11	259.01	4.09E-4	-16	100°+26mT
34X-1, 33	259.73	1.21E-3	-80	100°+16mT
34X-1, 86	260.26	4.31E-4	-82	100°+10mT
35X-1, 58	264.98	1.16E-3	-73	460°
35X-2, 18	266.08	1.13E-3	-39	250°+30mT
35X-2, 107	266.97	8.31E-4	-20	250°+20mT
35X-3, 35	267.75	7.48E-4	0	250°+30mT
35X-3, 105	268.45	8.74E-4	-2	250°+30mT
35X-4, 42	269.32	1.11E-3	-20	250°+30mT
35X-4, 118	270.08	9.45E-4	-50	250°+30mT
35X-5, 68	271.08	1.45E-3	-54	250°+30mT
35X-5, 135	271.75	5.21E-4	-4	250°+20mT
37X-1, 66	279.56	6.26E-4	-33	250°+20mT
37X-1, 145	280.35	2.67E-4	-29	250°+10mT
37X-2, 68	281.08	6.62E-4	-69	250°+15mT
37X-2, 116	281.56	1.97E-4	0	250°+10mT
37X-3, 28	282.18	1.18E-3	-10	400°

Note: The NRM column represents the initial NRM intensity of each sample and the demagnetization step column refers to the highest step attained during the treatment of each sample.

Appendix C. Directions of characteristic magnetization of Triassic sediments in Hole 760B.

Sample (core, section, cm)	Depth (mbsf)	NRM (A/m)	Inclination (°)	Demagnetization step
122-760B-				
6R-1, 35	283.35	9.10E-5	+30	150°+30mT
6R-1, 113	284.13	1.96E-4	+23	210°
6R-2, 32	284.82	1.63E-3	+30	250°+15mT
6R-2, 86	285.36	1.26E-4	-13	210°
7R-1, 21	292.71	6.91E-4	+29	100°+35mT
7R-1, 120	293.70	2.49E-4	+37	100°+30mT
7R-2, 17	294.17	4.84E-4	+28	100°+35mT
7R-2, 131	295.31	3.58E-4	-47	210°+10mT
8R-1, 35	302.35	2.74E-3	+28	210°+30mT
8R-1, 121	303.21	4.24E-4	-12	210°
8R-2, 32	303.82	6.40E-5	-24	210°
8R-2, 105	304.55	2.86E-4	-33	250°+22mT
8R-3, 34	305.34	8.90E-5	-12	210°
9R-1, 17	311.67	2.98E-4	+58	210°+10mT
9R-1, 128	312.78	2.27E-3	+22	250°+45mT
9R-2, 130	314.30	8.10E-5	+36	210°
9R-3, 116	315.66	4.63E-4	+4	210°+25mT
10R-1, 107	322.07	1.34E-3	+20	210°+30mT
10R-2, 62	323.12	9.98E-4	+27	210°+30mT
10R-2, 131	323.81	6.80E-4	+37	210°+30mT
11R-2, 95	332.95	1.25E-3	+17	210°+10mT
11R-3, 94	334.44	5.76E-4	+16	210°+10mT
12R-1, 81	340.81	1.43E-4	+28	100°+10mT
12R-1, 108	341.08	1.61E-4	-11	100°+10mT
12R-2, 50	342.00	1.65E-4	+7	100°+15mT
12R-2, 100	342.50	2.04E-4	+35	100°+35mT
12R-3, 60	343.60	1.02E-3	+15	100°+35mT
13R-1, 56	350.06	3.62E-3	+30	100°+25mT
13R-1, 97	350.47	7.74E-4	+27	150°
14R-1, 87	359.87	1.50E-3	+8	210°+30mT
14R-3, 103	363.03	4.22E-4	+17	210°+25mT
14R-4, 84	364.34	2.67E-4	-21	210°
16R-1, 77	378.77	4.70E-5	-42	210°+10mT
16R-2, 77	380.27	4.87E-4	+28	210°+30mT
16R-3, 58	381.58	1.29E-3	-21	250°+45mT
16R-4, 23	381.73	5.47E-3	-24	210°+30mT
16R-4, 83	382.33	5.17E-3	-23	210°+35mT
17R-2, 130	390.30	2.45E-4	-21	100°+20mT
17R-3, 42	390.93	5.64E-4	-2	100°+35mT
18R-1, 133	398.33	6.25E-4	-9	210°+20mT
18R-2, 86	399.36	1.12E-3	-33	210°+30mT
19R-1, 84	407.34	1.43E-3	-46	210°+30mT
19R-2, 12	408.12	3.41E-3	-20	210°+30mT
19R-3, 42	409.92	7.57E-4	-16	210°+20mT
19R-3, 127	410.77	1.14E-3	-7	210°+25mT
19R-4, 131	412.31	4.69E-4	-33	210°+35mT
20R-1, 113	417.13	1.25E-3	-6	210°+35mT
20R-2, 53	418.03	1.11E-3	-13	210°+35mT
20R-2, 127	418.77	1.24E-3	-7	210°+35mT
20R-3, 56	419.56	7.30E-4	-12	210°+35mT
20R-3, 126	420.26	9.06E-4	+9	210°+10mT

Appendix C (continued).

Sample (core, section, cm)	Depth (mbsf)	NRM (A/m)	Inclination (°)	Demagnetization step
20R-4, 57	421.07	1.44E-3	0	210°+20mT
20R-4, 130	421.80	9.55E-4	-29	210°+30mT
20R-5, 66	422.66	1.93E-3	-33	250°+35mT
21R-1, 34	425.84	3.49E-4	-24	210°+10mT
21R-1, 89	426.39	2.20E-4	+9	210°+10mT
21R-2, 65	427.65	5.82E-4	-17	210°+20mT
21R-2, 125	428.25	4.61E-4	-8	210°+20mT
21R-3, 66	429.16	7.25E-4	-68	210°+10mT
21R-3, 124	429.74	1.07E-3	-21	210°+30mT
21R-4, 65	430.65	2.31E-4	-19	210°+10mT
22R-1, 24	435.24	6.70E-5	-4	210°
22R-1, 101	436.01	3.24E-4	+2	210°
22R-2, 45	436.95	4.14E-4	0	210°+30mT
22R-2, 139	437.89	3.68E-4	+5	210°
22R-3, 49	438.49	7.61E-4	-10	210°+30mT
22R-3, 103	439.03	4.98E-4	+14	210°+20mT
22R-4, 42	439.92	6.06E-4	-54	210°+30mT
22R-4, 146	440.96	6.04E-4	-30	200°
23R-1, 55	445.05	4.31E-4	-53	210°+30mT
23R-1, 122	445.72	4.48E-4	-56	210°+35mT
23R-2, 25	446.26	1.31E-3	-46	210°+30mT
23R-2, 130	447.30	6.72E-4	-44	210°+20mT
23R-3, 27	447.77	1.02E-3	-38	210°+35mT
23R-3, 112	448.62	5.98E-4	-24	210°+35mT
23R-4, 37	449.37	8.70E-4	+39	210°+25mT
23R-4, 132	450.32	5.91E-4	+7	210°+30mT
25R-2, 72	465.72	4.71E-4	-16	100°+35mT
27R-1, 30	477.80	1.66E-4	-9	210°+35mT
27R-1, 133	478.83	6.77E-4	-1	210°+35mT
27R-2, 17	479.17	3.92E-4	+9	210°+30mT
27R-2, 135	480.35	5.34E-4	+8	210°+35mT
27R-3, 27	480.72	6.52E-4	+19	250°+15mT
27R-3, 135	481.85	5.74E-4	+6	210°+35mT
27R-4, 22	482.22	6.01E-4	-10	210°+30mT
27R-4, 131	483.31	7.51E-4	-16	210°+35mT
27R-5, 143	484.93	5.67E-4	-3	210°+35mT
27R-6, 122	486.22	4.90E-4	+4	210°+35mT
27R-6, 142	486.42	4.59E-4	-9	210°+25mT
28R-1, 36	487.36	1.64E-3	-6	210°+30mT
28R-2, 36	488.86	7.70E-4	-8	210°+30mT
28R-3, 18	490.18	5.64E-4	-5	210°+30mT
28R-4, 73	492.23	7.75E-4	-5	250°
29R-1, 36	496.86	8.48E-4	-13	210°+25mT
29R-1, 94	497.44	8.62E-4	-5	210°+30mT
29R-2, 72	498.72	6.48E-4	-10	210°+30mT
29R-2, 143	499.43	1.20E-3	+12	210°+30mT
29R-3, 53	500.03	4.74E-4	+11	210°+10mT
29R-3, 130	500.80	9.82E-4	-60	210°+10mT
29R-4, 41	501.41	7.98E-4	+4	210°+30mT

Note: The NRM column represents the initial NRM intensity of each sample and the demagnetization step column refers to the highest step attained during the treatment of each sample.

Appendix D. Directions of characteristic magnetization of Triassic sediments in Hole 761C.

Sample (core, section, cm)	Depth (mbsf)	NRM (A/m)	Inclination (°)	Demagnetization step
122-761C-				
23R-1, 146	338.66	6.80E-5	-32	250°
23R-2, 28	338.98	1.30E-5	—	
23R-2, 130	340.00	2.20E-5	—	
23R-3, 44	340.64	3.40E-5	-67	150°
23R-3, 114	341.34	6.20E-5	-40	250°
23R-4, 67	342.37	1.02E-4	-5	250°
24R-1, 16	346.86	1.40E-5	-32	250°
24R-1, 127	347.97	2.20E-5	—	
24R-2, 38	348.58	1.01E-4	+48	250°
24R-2, 139	349.59	3.60E-5	+25	180°
24R-3, 24	349.94	3.80E-5	-58	210°
25R-1, 87	358.57	1.49E-4	+39	250°
26R-1, 58	366.28	1.16E-4	+45	300°
26R-1, 135	367.05	1.24E-4	+12	250°
26R-2, 18	367.38	2.27E-4	+42	250°
26R-2, 52	367.72	2.10E-5	+42	250°
26R-3, 58	369.28	9.40E-5	+44	300°
26R-3, 107	369.77	4.80E-5	+18	250°
26R-4, 90	371.10	5.50E-5	+29	300°
26R-5, 86	372.56	4.90E-5	+9	300°
26R-6, 94	374.14	2.30E-5	+11	300°
29R-1, 28	389.48	9.40E-5	-38	400°
29R-1, 95	390.15	1.72E-4	-30	300°
30R-1, 95	399.65	2.65E-4	-28	100°+15mT
30R-2, 22	400.42	1.52E-4	-4	100°+15mT
30R-2, 110	401.30	8.22E-4	-36	300°
31R-1, 49	408.69	4.80E-5	-49	150°
31R-1, 144	409.64	7.90E-5	+29	100°+15mT
31R-2, 117	410.87	2.06E-4	+8	100°+20mT
31R-3, 90	412.10	5.30E-5	+17	100°+25mT
31R-4, 16	412.86	1.92E-4	+28	400°
31R-4, 142	414.12	5.28E-4	-69	300°
31R-5, 11	414.31	2.98E-4	+9	300°
32R-1, 30	418.00	3.30E-5	+6	220°
32R-1, 136	419.06	2.29E-4	-50	300°
32R-2, 47	419.67	1.44E-4	-40	300°
32R-2, 118	420.38	5.40E-5	+67	300°
32R-3, 45	421.15	1.14E-3	-45	300°
32R-3, 104	421.74	1.57E-3	-43	400°
33R-1, 50	427.70	5.70E-5	+22	100°+15mT
33R-1, 126	428.46	1.79E-4	+20	100°+25mT
33R-2, 21	428.91	3.30E-4	-2	100°+15mT

Note: The NRM column represents the initial NRM intensity of each sample and the demagnetization step column refers to the highest step attained during the treatment of each sample.